EINSTEIN OBSERVATIONS OF THE SNRs IC443, W44 AND W49B

M.G.Watson, R.Willingale, J.P.Pye, D.P.Rolf, N.Wood, and N.Thomas
X-Ray Astronomy Group, University of Leicester, England.

F.D.Seward
Center for Astrophysics, Cambridge, Ma., USA.

We present soft x-ray observations made with the Einstein Observatory Imaging Proportional Counter (IPC) of IC443, W44 and W49B (for details of the observatory and instruments see Giacconi et al.1979) . The x-ray emission from IC443 and W44 is clearly concentrated within the interior of the remnant with little or no evidence for a limb-brightened shell. Significant spectral differences are found across the x-ray images in both remnants which are interpreted as being due to a combination of differential absorption by molecular clouds and intrinsic spatial temperature variations. The distant remnant W49B is only just resolved in the IPC observations, but additional observations with the High Resolution Imager (HRI) indicate a similar "infilled" morphology to IC443 and W44.

IC443

The old supernova remnant IC443 shows a partial shell structure at radio wavelengths, brightest in the NE, together with a complex system of optical filaments which display a detailed correlation with the radio emission (e.g. Duin and Van der Laan 1975). Studies at millimetre wavelengths have revealed a dense CO cloud associated with IC443, which lies across the centre of the remnant (Cornett et al.1977, Scoville at al.1977). Early x-ray studies (e.g. Malina et al.1976) indicated an age $< 10^4$ years, in disagreement with much larger estimates from the observed low ($\sim$ 100 km s^{-1}) expansion velocity of the optical filaments. The distance to IC443 is not well determined with estimates in the range 0.5 to 2.5 kpc; we adopt d = 2 kpc.

In Fig.1 we show the soft x-ray image of IC443 overlaid on an optical plate of the remnant. The x-ray image is a composite of three overlapping observations with a total integration time of 5.1 ksec. The results are summarised in Table 1. There is evident correlation with the optical emission. Highest x-ray surface brightness occurs in the NE quadrant, but the x-ray emission appears to originate predominantly from the interior of the remnant. No significant emission is seen outside

J. Danziger and P. Gorenstein (eds.), Supernova Remnants and their X-Ray Emission, 273–280.
© 1983 by the IAU.

https://doi.org/10.1017/S0074180900033994 Published online by Cambridge University Press

Table 1 Summary of results

	IC443	W44	W49B
Assumed distance d [kpc]	2	3	10
Spectrum[1]: T_x [10^7K]	2	2	2
(assumed) N_H [10^{21} cm^{-2}]	4	5	30
Luminosity[2] [10^{35} erg s^{-1}]	2.5	1.6	12
Maximum dimensions [arcmin]	50	25 x 35	6
[pc]	29	22 x 31	18
Electron density[3] $\langle n_e \rangle$ [cm^{-3}]	0.15	0.2	1
Total emitting mass[4] [$M_\odot$]	60	60	85
Total thermal energy[4] [10^{50} ergs]	4	4	7

Notes

(1) Approximate spectral fit to the IPC data with an optically thin thermal spectrum following Raymond and Smith (1977).
(2) Intrinsic source luminosity [0.5 - 4.5 keV] corrected for absorbing column density.
(3) Derived electron density assuming emissivities for fitted spectrum. Note that a volume filling factor f = 1 has been assumed. For different filling factors and source distances $n_e \propto f^{-\frac{1}{2}} d^{-\frac{1}{2}}$.
(4) Total emitting mass and thermal energy content for f=1. Both quantities scale as $f^{\frac{1}{2}} d^{\frac{5}{2}}$.

(The values quoted in Table 1 assume cosmic abundances and ionisation equilibrium. The inclusion of enhanced metal abundances and non-equilibrium ionisation (e.g. Gronenschild & Mewe 1982 and several contributors to this volume) can make substantial differences to the temperature and density values and would tend to lower the total mass and thermal energy estimates.)

the edge of the remnant as defined by the radio/optical boundary (except possibly in the NW), and profiles through the x-ray image confirm that there is no appreciable limb-brightening except in part of the NW quadrant.

The spectral parameters derived for IC443 (quoted in Table 1) are necessarily crude since the energy resolution of the IPC allows a wide range of temperature and column density values. Assuming $N_H = 4 \times 10^{21}$ cm^{-2} (cf. Malina et al.1976), the approximate x-ray temperature

https://doi.org/10.1017/S0074180900033994 Published online by Cambridge University Press

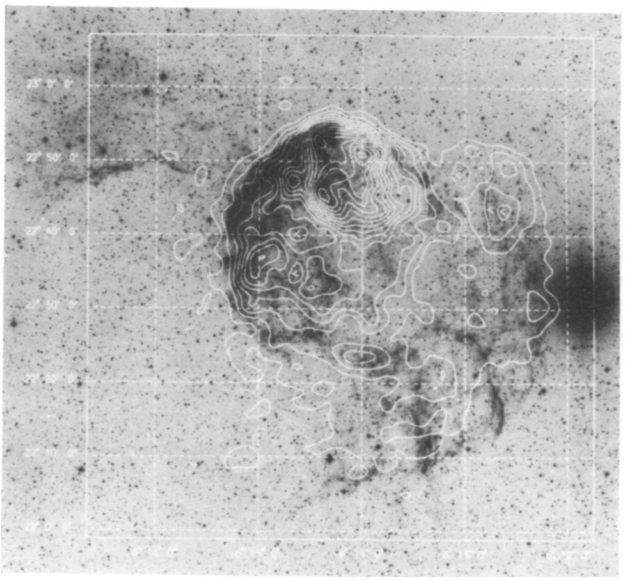

Fig.1 IPC x-ray image of IC443 (shown as contour map linear in x-ray surface brightness) overlaid on the PSS red plate. The x-ray image [~ 0.5 - 3 keV] has been Wiener filtered.

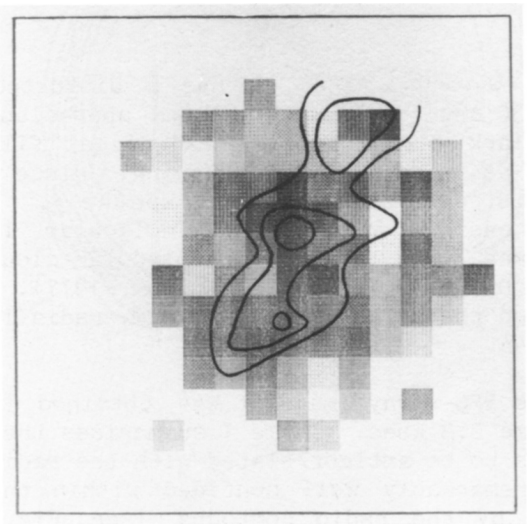

Fig.2 Spectral hardness map for IC443 (shown as linear greyscale) together with CO emission contours based on Cornett et al. (1977) shown to the same scale a Fig.1. Hardness ratio plotted is [counts in 1.3 - 3.1 keV band] / [counts in 0.2 - 1.3 keV band] for 256 arcsec. pixels.

https://doi.org/10.1017/S0074180900033994 Published online by Cambridge University Press

2×10^7 K is somewhat higher than quoted by previous investigators (e.g. Galas et al.1981, Charles et al.1981). Nevertheless more detailed analysis of the IPC spectra for 5 regions inside IC443 confirms our approximate parameters.

In order to look for spectral variations across the x-ray image we have constructed a map of the hardness ratio (shown in Fig.2). (Note that changes in the hardness ratio can be due to either increased low energy absorption or increased x-ray temperatures, or both). Over the central region of the image there is clearly reasonable correlation of the hardness ratio with the CO emission contours (also shown in Fig.2), indicating increased low energy absorption in the dense molecular cloud. For $T_x \approx 2 \times 10^7$ K the hardness ratios observed in the region of the molecular cloud correspond to an additional column density of $\sim (5 - 10) \times 10^{21}$ cm^{-2} through the cloud, consistent with density estimates from the CO measurements (Cornett et al.1977, Scoville et al.1977). Significant hardness variations are seen over other parts of the remnant which are probably not affected by localised absorption (on the basis of the CO map). The outer edges of the x-ray emission, in particular the brightest region to the N, have on average lower hardness ratios indicating lower temperatures ($\lesssim 5 \times 10^6$ K). The average x-ray spectra for IC443 quoted by Charles et al.(1981) and Galas et al.(1981) are consistent with this lower temperature (although it is clear from the IPC results that a single spectrum cannot be expected to be a good representation of the x-ray emission).

W44 (G34.6-0.5)

Radio maps of W44 show that it has a distorted shell structure approximately 20 x 30 arcmin. in extent with appreciable flattening in the NE (e.g. Clark et al.1975). No optical filaments have been detected, possibly as a result of reddening, since the (kinematic) distance to W44 is estimated to be 3 kpc (e.g. Radhakrishnan et al.1972). In the eastern part of W44 molecular line observations indicate the presence of a large dense molecular cloud associated with the remnant (e.g. Dickel et al.1976, Wooten 1977). Knapp and Kerr (1974) have reported the detection of a large, radially expanding shell of HI surrounding W44.

Fig.3 shows the IPC x-ray image of W44 obtained in an observation with integration time 2.3 ksec. Table 1 summarises the results. The x-ray emission appears to be anticorrelated with the radio emission in the sense that it is remarkably well confined within the boundary of the remnant as defined by the radio contours (see Fig.3). The x-ray emission is very clearly "centre-brightened" rather than limb-brightened, and significantly elongated in the N-S direction by about the same amount as the radio shell. Spectral parameters for W44 are quoted in Table 1. Note that in order to obtain a reasonable temperature estimate from the IPC spectrum, a column density of 5×10^{21} cm^{-2} appropriate for d = 3 kpc (e.g. Seward et al.1972) was assumed.

https://doi.org/10.1017/S0074180900033994 Published online by Cambridge University Press

As for IC443 we have looked for spectral variations across the x-ray image by constructing a spectral hardness map. Significant hardness variations are seen, with the hardest region occurring in the NE near the peak of the radio emission, but there is no obvious correlation either with x-ray morphology, or the CO emission contours (e.g. Wooten 1977). If we assume that the emission from W44 is isothermal, the observed hardness variations correspond to the absorbing column density varying between 10^{20} to 10^{22} cm^{-2}. Alternatively, assuming a uniform column density of 5 x 10^{21} cm^{-2} would imply temperatures ranging from 10^{7} to greater than 10^{8} K. Because the implied range of column densities is so large, we suspect that most of the observed hardness variations are due to significant temperature differences in the emission region, although the increased hardness ratio in the NE could be due to increased absorption originating in the molecular cloud.

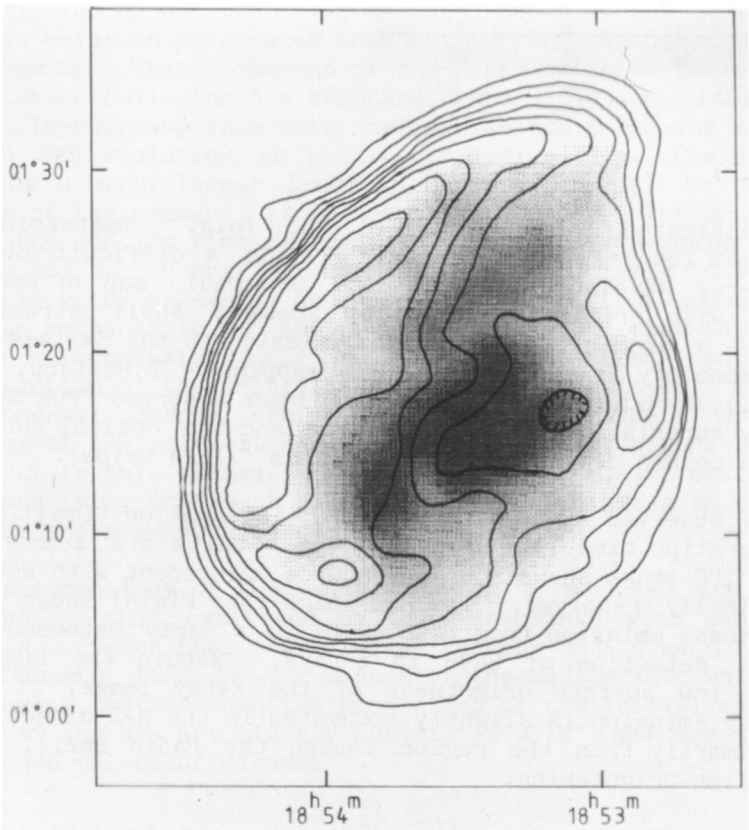

Fig.3 IPC x-ray image of W44 together with radio contours taken from the 408 MHz map of Clark et al.(1975) (HPBW ≈ 3 arcmin.). The x-ray image [∼0.5 - 4 keV] has been smoothed with a 30 arcsec. Gaussian. The greyscale is linear in x-ray surface brightness.

https://doi.org/10.1017/S0074180900033994 Published online by Cambridge University Press

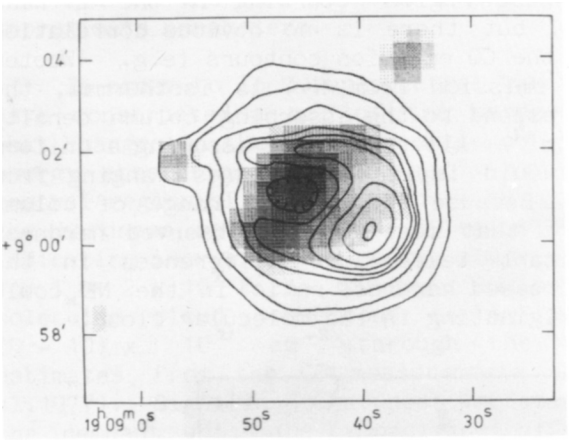

Fig.4 HRI x-ray image of W49B together with radio contours taken from the 10.7 GHz map of Downes & Wilson (1974) (HPBW = 1.3 arcmin.). The x-ray image [$\sim$ 0.2 - 4 keV] has been smoothed with a 30 arcsec. Gaussian. The greyscale is linear in x-ray surface brightness.

W49B (G43.3-0.2)

At an estimated distance of 10 kpc (e.g. Radhakrishnan et al.1972), and at low galactic latitude, W49B is a difficult object to observe at x-ray wavelengths. The 10.7 GHz radio map of Downes and Wilson (1974) with arcminute resolution shows a shell structure of diameter $\sim$ 3 - 4 arcmin. with enhanced emission in the SW (see Fig.4). (The shell morphology is confirmed by VLA mapping - D.Helfand, private communication.) Optical emission has not been observed from W49B, but this is hardly surprising given the distance and the optical absorption expected for a column density $N_H \approx 3 \times 10^{22}$ cm^{-2} (see below).

W49B was observed both with the IPC (integration time 1.6 ksec.) and HRI (integration time 11.1 ksec.). The results are summarised in Table 1. The IPC image shows a bright source coincident with W49B which is only marginally resolved. The HRI image (see Fig.4) shows very low surface brightness emission from W49B which is clearly extended. This is the first detection of W49B in x-rays. Within the limitations imposed by the low surface brightness of the x-ray image, it appears that the x-ray emission is slightly elongated in the N-S direction, and originates primarily from the region inside the radio shell, with no evidence for limb-brightening.

As with IC443 and W44, the IPC data can be used to obtain approximate spectral parameters for the remnant (see Table 1), although the angular resolution of the IPC is too low to allow examination of spectral variations over the image. The observed HRI flux is particularly sensitive to the absorbing column density and has been used as an additional constraint on the spectral parameters. The derived column density agrees well with the value estimated from HI 21 cm measurements (e.g. Akabane & Kerr 1965; Radhakrishnan et al.1972).

https://doi.org/10.1017/S0074180900033994 Published online by Cambridge University Press

CONCLUSION : RADIO SHELLS AND X-RAY INTERIORS

The Einstein observations of IC443, W44 and W49B clearly show that in each case the x-ray emission is concentrated within the interior of the remnant with little or no evidence for limb-brightening. The lack of observed limb-brightening is easily understood if the shells are cool ($\sim 10^6$ K) since the attenuation by moderate column densities for low temperature thermal emission is large enough to hide the emission in the IPC. This explanation is particularly attractive for IC443 where there is some evidence (see above) for such a cool shell. Low x-ray shell temperatures are consistent with the estimated ages ($\gtrsim 10^4$ years) of both IC443 and W44, but may be problematic for W49B which is probably somewhat younger.

As there is no evidence for a central pulsar to power the interior x-ray emission by non-thermal processes, the simplest interpretation is that this emission originates in a hot ($\sim 10^7$ K) thermal plasma filling the remnants. This component of the x-ray emission is not expected for SNR evolution following the standard Sedov solution, in which most of the mass is swept-up in a thin shell which dominates the x-ray emission. Although SNR evolution in a "cloudy" medium (e.g. Cowie & McKee 1977) may allow a much larger fraction of the material to remain in the interior of the remnant, it is not clear how the interior can be heated. Because the cooling time is long, the emission seen could be interpreted as a fossil of an original hot plasma created early in the life of the remnant (e.g. by a reverse shock), but we note that x-ray observations of young remnants (e.g. SN1006, Pye et al.1981) show that the interior emission is dominated by a relatively cool plasma containing only a small fraction of the initial supernova energy release. In contrast the total thermal energy estimates (Table 1) indicate that appreciable fractions of the initial energy (i.e $\sim 10^{51}$ ergs) of the supernovae are locked up in this plasma. The total emitting masses estimated are also large, and imply that most of the material originates in the ISM, rather than from the supernova ejecta.

The morphology of the x-ray emission from IC443 and W44 is quite different to that exhibited by other remnants with similar sizes and ages (e.g. Cygnus Loop and Vela). Perhaps one clue to understanding the difference lies in the nature of the medium into which the remnant is expanding, rather than the properties of the initial explosion, since both IC443 and W44 are closely associated with (and may be interacting with) dense molecular clouds.

The Einstein Observatory is funded by NASA. MGW,RW,JPP,NW and NT acknowledge financial support from the SERC, and MGW thanks the Royal Society for a travel support.

https://doi.org/10.1017/S0074180900033994 Published online by Cambridge University Press

REFERENCES

Akabane,K.,& Kerr,F.J.,1965. Aust.J.Phys.,18,91.
Charles,P.A.,Kahn,S.M.,Mason,K.O.,& Tuohy,I.R.,1981.
Ap.J.(Lett.),246,L121.
Clark,D.H.,Green,A.J.,& Caswell,J.L.,1975.
Aust.J.Phys.Ap.Suppl.,37,75.
Cornett,R.H.,Chin,G.,& Knapp,G.R.,1977. Astr.Astrophys.,54,889.
Cowie,L.L.,& McKee,C.F.,1977. Ap.J.,215,213.
Dickel,J.R.,Dickel,H.R.,& Crutcher,M.,1976. P.A.S.P,88,840.
Downes,D.,& Wilson,T.L.,1974. Astr.Astrophys.,34,133.
Duin,R.M.,& Van der Laan,H.,1975. Astr.Astrophys.,40,111.
Galas, C.M.F., Venkatesan, D.,& Garmire,G.,1981. Ap.J.,250, 216.
Giaconni,R., et al. 1979. Ap.J.,230 540.
Gronenschild, E.H.B.M., & Mewe,R.,1982. Astr. Astrophys.,48, 305.
Knapp, G.R., & Kerr, F.J.,1974. Astr.Astrophys. 33, 463.
Malina,R.,Lampton,M., & Bowyer, S.,1976. Ap.J.,207, 894.
Pye, J.P., Pounds, K.A., Rolf, D.P., Seward, F.D., Smith,A.,
& Willingale, R., 1981. M.N.R.A.S.194, 569.
Radhakrishnan,V., Goss,W.M., Murray,J.D., & Brooks, J.W., 1972.
Ap.J.Suppl., 24,49.
Scoville, N.Z, Irvine, W.M., Wannier, P.G., & Predmore, C.R., 1977.
Ap.J.,216, 320.
Seward, F.D., Burginyon, G.A., Grader, R.J., Hill, R.W., & Palmieri, T.M.
1972. Ap.J, 178, 131.
Wooten, H.A., 1977. Ap.J.,216, 440.

https://doi.org/10.1017/S0074180900033994 Published online by Cambridge University Press